Calculation of Solvation Free Energy from Quantum Mechanical Charge Density and Continuum Dielectric Theory

Mingliang Wang and Chung F. Wong*

Department of Chemistry and Biochemistry, University of Missouri-Saint Louis, One University Boulevard, Saint Louis, Missouri 63121

Received: November 10, 2005; In Final Form: February 20, 2006

We have combined ultrasoft pseudopotential density functional theory utilizing plane wave basis with a Poisson−Boltzmann/solvent-accessible surface area (PB/SA) model to calculate the solvation free energy of small neutral organic compounds in water. The solute charge density obtained from density functional theory was directly used in solving the Poisson−Boltzmann equation to obtain the reaction field. The polarized electronic wave function of the solute in the solvent was solved by including the reaction field in the density functional Hamiltonian. The quantum mechanical and Poisson−Boltzmann equations were solved self-consistently until the charge density and reaction field converged. Using the solute charge density directly instead of a point-charge representation permitted asymmetric distortion and spreading out of the electron cloud. Because the electron density could leave the van der Waals surface to penetrate into the high-dielectric solvent, the reaction field generated by this density was generally smaller than that obtained by using the point-charge representation. In applying this model to calculate the solvation free energy of 31 small neutral organic molecules spanning a range of 25 kcal/mol, we obtained a root-mean-square error of only 1.3 kcal/mol if we allowed one adjustable parameter to shift the calculated solvation free energy.

1. Introduction

Biochemical processes typically occur in the presence of solvent. Therefore, reliable modeling of biological structure and energetics requires the proper treatment of solvation effects. Explicit-solvent models describe the molecular details of the solvent but are expensive to use. Implicit-solvent models approximate the solvent as a dielectric continuum to significantly reduce the number of degrees of freedom. By avoiding extensive samplings of solvent configurations, implicit-solvent models are much cheaper to use.[1] Some widely used continuum solvent models include the Poisson−Boltzmann (PB) model,[2−7] the conductor-like screening model (COSMO),[8,9] the polarizable continuum model (PCM),[10,11] and the generalized Born (GB) model.[12−15] To improve the solvation free energy calculation, a broad range of continuum solvation models have been coupled with quantum mechanical methodologies. Most of the available methodologies have been described in a few recent reviews.[1,16−18]

This work focuses on using the PB approach, which is one of the most realistic continuum solvent models around. The PB equation can be solved numerically to take into account the complex shape of solute molecules. Common methods include the finite-difference and the boundary-element approaches.[4−6,17,19] In solving the PB equation, it is common to approximate the solute charge distribution by fixed atomic partial point charges. In combining the PB method with quantum mechanics, one can determine the partial point charges of a solute by fitting them to quantum mechanically derived electrostatic potential (ESP) to obtain ESP-fitted charges.[20] On the other hand, in combining a linear-scaling quantum mechanical method with the PB approach, Merz and co-workers employed scaled Mulliken and Coulson charges.[21] Although charges derived from ESP-fitting can be easily fed into a PB algorithm, their derivation depends somewhat on the choice of sampling points for calculating the ESP.[22,23] Directly using the charge density obtained from quantum calculation can eliminate this problem. This approach is explored in this work by applying it to calculate the solvation free energy of small organic molecules and comparing the results to those obtained by using point-charge and mixed point-charge/charge density representations.

Density functional theory is one of the most widely used methods in electronic structure calculations since Kohn and Sham proposed the first practical approach for obtaining numerical solutions.[24] In solid-state physics, the Kohn−Sham equation is now commonly solved by using the plane wave basis set, an ultrasoft or norm-conserving pseudopotential, and periodic boundaries.[25−27] Compared with local basis sets, the plane wave basis set offers advantages such as no basis set superposition error and no Pulay force. Basis set convergence can be controlled systematically by using only one parameter: the cutoff energy E_{cut}. On the other hand, one disadvantage of the plane wave basis set is that it requires a large number of plane waves to achieve convergence. However, the basis size can be dramatically reduced by using ultrasoft pseudopotential.[26,27] Practical use of the plane wave basis set also requires the application of periodic boundary conditions. When modeling an isolated molecule, the basic unit chosen needs to be large enough so that interactions between molecules in adjacent cells are negligible.[28] In the case of neutral systems with small dipole moments, satisfactory results can be obtained by using a relatively small basic simulation unit. For charged molecular systems or systems with large dipole moments, large errors can result from too small a basic calculation unit.[27] However, this difficulty can be overcome by a simple scheme proposed by Martyna and Tuckerman that utilizes a screen function in the long-range interaction terms.[29]

* Corresponding author. E-mail: wongch@umsl.edu.

10.1021/jp0565195 CCC: $33.50
Published on Web 03/21/2006

In this work, the electronic structure and total energy of a molecule were calculated by using the plane wave basis set together with an ultrasoft pseudopotential (PWPP).[25] The long-range interaction terms were treated with the screen function technique of Martyna and Tuckerman. Solvation effects were included by using the reaction field obtained from the solution of the PB equation. Because the PB equation was solved by using electron density or atomic partial charges derived from the quantum calculations, the Kohn−Sham and the PB equations needed to be solved iteratively until convergence was achieved. In this work, we used the finite-difference method of the University of Houston Brownian Dynamics (UHBD) program[2] to solve the PB equation with dielectric boundary defined by using Bondi radii.[30] We studied 31 neutral molecules and found good agreements with experimental data (root-mean-square error = 1.3 kcal/mol).

This paper is organized as follows: Section 2 describes the methods used to calculate the reaction field and the solvation free energy, and to couple the Kohn−Sham and the PB approaches. The Results and Discussion section follows. In this section, the results obtained by using charge density, fitted atomic partial point charges, and their hybrids are compared. Section 4 concludes.

2. Computational Methods

2.1. Kohn−Sham Equations with Ultrasoft Pseudopotentials and the Plane Wave Basis Set. The total energy functional of a system for a set of occupied electronic states can be written as[26,27]

$$E_{\mathrm{tot}} = \sum_i \left\langle \phi_i \right| -\frac{\hbar^2}{2m}\nabla^2 + V_{\mathrm{NL}} \left| \phi_i \right\rangle + E_{\mathrm{H}} + E_{\mathrm{xc}} + \int \mathrm{d}r V_{\mathrm{loc}}^{\mathrm{ion}}(\mathbf{r}) n(\mathbf{r}) \quad (1)$$

where V_{NL} and $V_{\mathrm{loc}}^{\mathrm{ion}}$ are the nonlocal and local operators of the ultrasoft pseudopotential, E_{H} and E_{xc} are the Hartree and exchange-correlation energies, respectively, and $n(\mathbf{r})$ is the electron density. The Kohn−Sham equation can be obtained by minimizing the total energy under the constraint of generalized orthonormality:

$$H|\phi_i\rangle = \epsilon_i S|\phi_i\rangle \quad (2)$$

where ϵ_i is the ith eigenvalue, S is a Hermitian overlap operator, and H is the Kohn−Sham Hamiltonian,

$$H = -\frac{\hbar^2}{2m}\nabla^2 + \sum_{nm,I} D_{nm}^{\mathrm{ion}} |\beta_n^{\mathrm{ion}}\rangle\langle\beta_m^{\mathrm{ion}}| + V_{\mathrm{loc}}^{\mathrm{ion}}(\mathbf{r}) + V_{\mathrm{H}}(\mathbf{r}) + V_{\mathrm{xc}}(\mathbf{r}) \quad (3)$$

where D_{nm}^{ion} is the "screened' coefficients defined in ref 27, and $|\beta_n^{\mathrm{ion}}\rangle\langle\beta_m^{\mathrm{ion}}|$ is the projector related to the ultrasoft pseudopotential. V_{H} is the Hartree potential, and V_{xc} is the exchange-correlation potential. Under the plane wave representation, the kinetic energy term is diagonal and the Hartree potential has a simple analytical form for periodic systems:

$$V_{\mathrm{H}}(\mathbf{G}) = \frac{4\pi}{\mathbf{G}^2} n(\mathbf{G}) \quad (4)$$

where $\mathbf{G}$ is the reciprocal lattice vector. As discussed earlier, the long-range Coulomb interactions between replicas can introduce errors in performing calculations for isolated systems. However, such errors can be reduced by introducing the screen function proposed by Martyna and Tuckerman in which the Hartree potential is written as[29]

$$V_{\mathrm{H}}(\mathbf{G}) = \frac{4\pi}{G^2} n(\mathbf{G}) + V_{\mathrm{screen}}(\mathbf{G}) \quad (5)$$

where $V_{\mathrm{screen}}(\mathbf{G})$ is obtained by taking the difference between the Fourier series and the Fourier transform of the long-range part of the Coulomb interactions. A similar scheme can be applied to the local potential $V_{\mathrm{loc}}^{\mathrm{ion}}(\mathbf{G})$. Finally, we used the Davison algorithm to solve the Kohn−Sham equation self-consistently by our modified plane wave self-consistent field (PWSCF) program.[25] The electron density or atomic partial charges fitted to the molecular ESP were used in the solution of the PB equation.

In our calculations, the minimum separation between adjacent periodic replicas was 20 Bohr. This separation distance combined with the use of screen function ensured that the error caused by neighboring images were negligible. To test the convergence of the plane wave basis set, reaction field energy G_{RF} was carried out by setting E_{cut} equal to 25 and 20 Rydberg for a water molecule. We found that the reaction field energy G_{RF} differed by only 0.1 kcal/mol. Therefore E_{cut} was chosen to be 20 Rydberg for all subsequent calculations. We also used the PBE functional in the solution of the Kohn−Sham equations.[31] In the least-squares fitting of the ESP charges, we followed previous work by utilizing sampling points between two surfaces constructed by using 1.2 and 1.7 times the van der Waals radii respectively.[22]

2.2. Numerical Solution of the PB Equation. The ESP can be obtained by solving the PB equation with a charge distribution $\rho(\mathbf{r})$:[32,33]

$$\nabla\cdot[\epsilon(\mathbf{r})\nabla\phi(\mathbf{r})] - \kappa^2(\mathbf{r})\phi(\mathbf{r}) = \rho(\mathbf{r}) \quad (6)$$

where $\epsilon(\mathbf{r})$ is the dielectric at $\mathbf{r}$, $\kappa(\mathbf{r})$ is the Debye−Hückel parameter, and $\phi(\mathbf{r})$ is the ESP. The UHBD program was used to calculate the ESP and the reaction field by using either the quantum mechanical charge density directly or ESP fitted charges.[2] If quantum mechanical charge density was used directly, the electron density $\rho(\mathbf{r})$ or ion valence charge Z_{ion} density expressed in each grid point of the real space PWSCF grid was first converted into a point charge. Then, a typical UHBD calculation was carried out, except this time atomic partial charges were replaced by point charges converted from each grid point in the PWSCF grid. This way, we have many more point charges than atomic point charges and some of these charges could be outside the dielectric boundary because the quantum mechanical charge density could extend beyond the dielectric surface surrounding the solute. In converting the charge density to a point charge, we multiplied the charge density at the grid point by the volume of a grid used in the UHBD calculation. We used a solvent-excluded surface generated by using a probe sphere of radius 1.4 Å to define the dielectric interface. Because electronic polarization was explicitly taken care of by the quantum calculations, the interior dielectric constant was set to 1. An exterior solvent dielectric constant of 80 was used. In all calculations presented here, $\rho(\mathbf{r})$ was set to zero, corresponding to a solution without salt. The Poisson equation was solved by using the incomplete Choleski decomposition method.[3]

The accuracy of the Poisson solution depends on the grid spacing used in the finite-difference method. For a water molecule, the reaction field energy G_{RF} obtained by using grid

spacings of 0.15 and 0.12 Å differed by only 0.04 kcal/mol. Therefore, when using the focusing method of Gilson and Honig[34] in solving the Poisson equation, we first calculated the ESP using a coarse grid with a dimension of 60^3 and a grid spacing of 0.5 Å, followed by a fine grid calculation with the same dimension but a smaller grid spacing of 0.15 Å. The Bondi radii were used in choosing surface points for ESP charge fitting and in defining the molecular surface (e.g., 1.20 Å for hydrogen, 1.70 Å for carbon, 1.52 Å for oxygen, 1.55 Å for nitrogen, and 1.80 Å for sulfur).[30]

2.3. Coupling between Kohn−Sham and PB Equations. We obtained the reaction field by solving the PB equation twice, once in the presence of the solvent, and once in a vacuum such that

$$\phi_{RF}(\mathbf{r}) = \bar{\phi}_{solvent}(\mathbf{r}) - \bar{\phi}_{vac}(\mathbf{r}) \quad (7)$$

The reaction field $\bar{\phi}(\mathbf{r})$ was incorporated into the Kohn−Sham Hamiltonian to give

$$H_{sol} = -\frac{\hbar^2}{2m}\nabla^2 + \sum_{nm,I} D_{nm}^{ion} |\beta_n^{ion}\rangle \langle \beta_m^{ion}| + V_{loc}^{ion}(\mathbf{r}) + V_H(\mathbf{r}) + V_{xc}(\mathbf{r}) + \phi_{RF}(\mathbf{r}) \quad (8)$$

Because the solution of the Kohn−Sham equation required the reaction field, the solution of which in turn depended on the quantum mechanically derived charge density (either used directly or in the form of ESP fitted charges), the Kohn−Sham and the PB equations were solved self-consistently until the total energy of the solute converged to within 10^{-8} Rydberg. In the solution of eq 8, the values of $\bar{\phi}_{RF}(\mathbf{r})$ on the Kohn−Sham equation grid were obtained from the PB equation grid using the trilinear interpolation formula, as in UHBD. In the self-consistent iteration procedure, one first performed a SCF calculation in a vacuum with a fixed solute geometry. The quantum mechanically derived charge density was then used in solving the PB equation to obtain the reaction field $\bar{\phi}_{RF}(\mathbf{r})$. $\bar{\phi}_{RF}(\mathbf{r})$ was then used in the following quantum mechanical calculation. This process was repeated until the solute energy converged. In these calculations, the solute geometry was obtained by optimizing it in a vacuum at the B3LYP/6−311 g** level using the Gaussian 03 package.[35]

2.4. Solvation Free Energy Calculations. With the quantum mechanically derived charge density, the solvation free energy was evaluated as follows:[21]

$$G_{sol} = G_{RF} + G_{wfd} + G_{np} \quad (9)$$

where G_{RF} is the interaction energy between the solute charge density and the reaction field $\bar{\phi}_{RF}(\mathbf{r})$, which was calculated by:

$$G_{RF} = \frac{1}{2}\int_V \rho(\mathbf{r})\bar{\phi}_{RF}(\mathbf{r})d\mathbf{r} + \frac{1}{2}\sum_A Z_v^A \bar{\phi}_{RF}(\mathbf{r}) \quad (10)$$

where Z_v^A is the ion valence charge. G_{wfd} is the energy resulting from the distortion of the solute wave function in going from vacuum to solution and is given by[20]

$$G_{wfd} = \sum_i [\langle \phi_i^s | H | \phi_i^s \rangle - \langle \phi_i^g | H | \phi_i^g \rangle] \quad (11)$$

Here, H is the Hamiltonian in the gas phase, ϕ_i^s was the ith solute orbital in solvent, and ϕ_i^g was the ith solute orbital in the gas phase. Finally, the nonpolar term G_{np} involved contributions from cavity formation and solute−solvent van der Waals interactions modeled as[20,36]

$$G_{np} = a + \sigma A \quad (12)$$

We treated a as an adjustable parameter to fit experimental results. A is the solvent-accessible surface areas. σ is a surface tension coefficient which was set to 0.006 kcal/mol Å^{-1}in our calculations.[37] As noticed in refs 38 and 39, eq 12 did not work as well for small organic molecules containing a ring. This limitation could be reduced by separating the nonpolar solvation free energy explicitly into dispersion and cavity terms, but more adjustable parameters are required.[40,41] Although we only used eq 12 in this paper, Levy et al.'s approach might further improve our model in the future.

TABLE 1: Calculated Solvation Free Energies of Cl$^-$ in Water (in kcal/mol)

ion	model[a]	G_{RF}	G_{wfd}	G_{SAS}[b]	G_{sol}	exptl
Cl^-	ρ/ρ	−79.75	2.11	0.51	−77.13	−73.4 ∼ −78.0
	ρ/q	−55.82			−53.20	
	q/ρ	−83.53	17.22		−65.81	
	q/q	−133.26			−115.54	

[a] Model ρ/ρ indicates that both the reaction field $\bar{\phi}(\mathbf{r})$ and G_{RF} were calculated by using the density ρ directly. In model ρ/q, the reaction field $\bar{\phi}(\mathbf{r})$ was calculated with ρ, whereas G_{RF} was evaluated with point charges derived by ESP fitting. Model q/ρ used fitted point charges in calculating the reaction field $\bar{\phi}(\mathbf{r})$, but used charge density in evaluating G_{RF}. In model q/q, the fitted point charges were used in calculating the reaction field $\bar{\phi}(\mathbf{r})$ as well as G_{RF}. [b] G_{SAS} was calculated by multiplying the solvent-accessible surface area by 0.006.

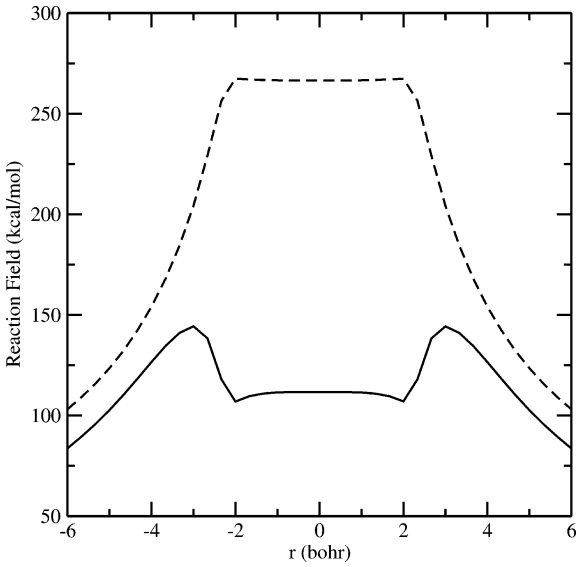

Figure 1. Reaction field $\bar{\phi}(\mathbf{r})$ from the solution of the Poisson equation for Cl$^-$. The solid line was obtained by using the charged density obtained from density functional calculation. The dashed line was obtained by using a single point charge of unit one at the atom center.

3. Results and Discussion

Because most previous PB calculations employed atomic partial charges rather than charge density, we compared four different calculational models constructed by using charge density alone, ESP-fitted charges alone, and their hybrids: In the ρ/ρ model, the reaction field $\bar{\phi}(\mathbf{r})$ was obtained from the PB equation using the charge density, and the reaction field energy G_{RF} was also calculated by using the density ρ in eq 10. In the ρ/q model, the reaction field energy G_{RF} was evaluated by using ESP-fitted charges in eq 10. In the q/ρ model, the ESP-fitted charges were used in the solution of the PB equation,

TABLE 2: Experimental and Calculated Solvation Free Energies for 31 Small Neutral Molecules in Water (in kcal/mol)

molecule	model[a]	G_{RF}	G_{wfd}	G_{SAS}[b]	G_{np}	G_{sol}	exptl	molecule	model[a]	G_{RF}	G_{wfd}	G_{SAS}[b]	G_{np}	G_{sol}	exptl
methanethiol	ρ/ρ	−5.38	0.95	1.09	2.63	−1.80	−1.24	methyl ethyl	ρ/ρ	−5.97	1.16	1.50	3.03	−1.79	−1.49
	ρ/q	−3.53			1.70	−0.88		sulfide	ρ/q	−4.16			2.10	−0.91	
	q/ρ	−3.91	1.16		1.72	−1.04			q/ρ	−4.60	1.37		2.12	1.12	
	q/q	−4.38			2.50	−0.73			q/q	−4.97			2.90	−0.71	
methanol	ρ/ρ	−7.67	1.31		2.50	−3.86	−5.11	4-cresol	ρ/ρ	−9.19	1.36	1.64	3.17	−4.66	−6.13
	ρ/q	−7.03			1.57	−4.15			ρ/q	−8.44			2.24	−4.85	
	q/ρ	−7.23	1.45		1.59	−4.19			q/ρ	−8.82	1.63		2.26	−4.93	
	q/q	−7.67			2.37	−3.85			q/q	9.71			3.04	−5.04	
phenol	ρ/ρ	−9.55	1.50	1.55	3.08	−4.98	−6.60	4-methyl-	ρ/ρ	−15.52	3.90	1.44	2.97	−8.65	−10.25
	ρ/q	−8.67			2.15	−5.03		imidazole	ρ/q	−14.46			2.04	−8.51	
	q/ρ	−9.06	1.77		2.17	−5.12			q/ρ	−15.09	4.37		2.06	−8.66	
	q/q	−9.82			2.95	−5.11			q/q	−16.35			2.84	−9.13	
acetic acid	ρ/ρ	−12.31	1.90	1.22	2.75	−7.66	−6.70	3-methyl-	ρ/ρ	−10.16	1.73	1.89	3.42	−5.01	−5.91
	ρ/q	−11.90			1.82	−8.18		indole	ρ/q	−8.59			2.49	−4.37	
	q/ρ	−12.15	2.08		1.84	−8.23			q/ρ	−9.35	2.18		2.51	−4.66	
	q/q	−12.70			2.62	−8.00			q/q	−10.20			3.29	−4.72	
H_2O	ρ/ρ	−10.09	1.76	0.73	2.26	−6.07	−6.30	*n*-butylamine	ρ/ρ	−7.50	1.39	1.42	2.95	−3.16	-4.29
	ρ/q	−9.53			1.33	−6.44			ρ/q	−6.56			2.02	−3.15	
	q/ρ	−9.80	1.96		1.35	−6.49			q/ρ	−6.82	1.57	2.04		−3.21	
	q/q	−10.03			2.13	−5.93			q/q	−7.90	2.82	−3.51			
benzene	ρ/ρ	−4.12	0.54	1.45	2.98	−0.60	−0.9	*n*-propyl-	ρ/ρ	−22.31	4.26	1.82	3.35	−14.70	−10.91
	ρ/q	−3.21			2.05	−0.62		guanidine	ρ/q	−18.40			2.42	−11.72	
	q/ρ	−3.53	0.77		2.07	−0.68			q/ρ	−20.18	4.69		2.44	−13.05	
	q/q	−4.01			2.85	−0.39			q/q	−20.45			3.22	−12.54	
methane	ρ/ρ	−0.94	0.03	0.84	2.37	1.47	1.93	aniline	ρ/ρ	−9.30	1.46	1.45	2.98	−4.86	−5.49
	ρ/q	−0.49			1.44	0.98			ρ/q	−8.59			2.05	−5.07	
	ρ	−0.51	0.04		1.46	0.99			q/ρ	−9.15	1.77		2.07	5.31	
	q/q	−0.61			2.24	1.68			q/q	−10.14			2.85	−5.52	
propionic	ρ/ρ	−10.72	1.58	1.36	2.89	−6.24	−6.47	NH_3	ρ/ρ	−8.58	1.76	0.81	2.34	−4.47	−4.29
acid	ρ/q	−9.79			1.96	−6.24			ρ/q	−8.03			1.41	-4.86	
	q/ρ	−9.98	1.73		1.98	−6.27			q/ρ	−8.39	2.03		1.43	−4.92	
	q/q	−10.42			2.76	−5.94			q/q	−9.29			2.21	−5.05	
acetone	ρ/ρ	−10.16	2.33	1.32	2.85	−4.99	−3.90	methylamine	ρ/ρ	−7.66	1.48	1.02	2.55	-3.63	-4.50
	ρ/q	−9.51			1.92	−5.27			ρ/q	−6.56			1.62	−3.45	
	q/ρ	−9.72	2.54		1.94	−5.24			q/ρ	−6.80	1.63		1.64	−3.52	
	q/q	−10.14			2.72	-4.89			q/q	−7.71			2.42	−3.65	
butane	ρ/ρ	−1.56	0.04	1.45	2.98	1.46	2.15	acetonitrile	ρ/ρ	−13.56	3.45	1.05	2.58	−7.53	−3.90
	ρ/q	−0.23			2.05	1.86			q/ρ	−13.64			1.65	−8.54	
	q/ρ	−0.27	0.03		2.07	1.83			q/ρ	−14.32	4.12		1.67	−8.53	
	q/q	−0.33			2.85	2.54			q/q	−15.47			2.45	-8.90	
acetamide	ρ/ρ	−16.59	3.83	1.27	2.80	−9.97	−9.71	pyridine	ρ/ρ	−8.54	1.88	1.33	2.86	−3.80	−4.70
	ρ/q	−16.15			1.87	−10.45			ρ/q	−7.57			1.93	−3.75	
	q/ρ	−16.47		4.10	1.89	−10.49			q/ρ	−8.09	2.29		1.95	−3.84	
	q/q	−17.26			2.67	−10.49			q/q	−9.40			2.73	−4.37	
i-butane	ρ/ρ	−1.70	0.05	1.46	2.99	1.35	2.30	1-methyl-	ρ/ρ	−28.41	7.17	1.70	3.23	−18.02	−18.40
	ρ/q	−0.54			2.06	1.57		cytosine	ρ/q	−26.94			2.30	−17.48	
	q/ρ	−0.57	0.06		2.08	1.57			q/ρ	−28.39	7.96		2.32	−18.11	
	q/q	−0.67			2.86	2.26			q/q	−29.46			3.10	−18.39	
propionamide	ρ/ρ	−15.69	3.65	1.43	2.96	−9.09	−9.41	1-methyl-	ρ/ρ	−20.55	4.65	1.63	3.16	−12.74	−14.0
	ρ/q	−14.86			2.03	−9.18		uracil	ρ/q	−21.35		2.23	−14.47		
	q/ρ	−14.98	3.80		2.05	−9.13			q/ρ	−19.49	4.62	2.25	−12.61		
	q/q	−15.72			2.83	−9.10			q/q	−21.74		3.03	−14.08		
ethanol	ρ/ρ	−7.74	1.31	1.22	2.75	−3.68	−5.01	9-methyl-	ρ/ρ	−31.97	7.33	1.94	3.47	−21.17	−22.4
	ρ/q	−6.89			1.82	−3.76		guanine	ρ/q	−30.55			2.54	−20.69	
	q/ρ	−7.05	1.42		1.84	−3.80			q/ρ	−32.73	8.61		2.56	−21.56	
	q/q	−7.32			2.62	−3.29			q/q	−34.50			3.34	−22.55	
ethanethiol	ρ/ρ	−5.65	1.02	1.30	2.83	−1.79	−1.30	9-methyl-	ρ/ρ	−21.50	3.49	1.87	3.41	−14.60	−13.6
	ρ/q	−3.71			1.90	−0.78		adenine	ρ/q	−18.79			2.48	−12.84	
	q/ρ	−4.09	1.26		1.92	−0.90			q/ρ	−19.82	3.88		2.50	−13.45	
	q/q	−4.52			2.70	−0.56			q/q	−21.11			3.28	−13.95	
toluene	ρ/ρ	−4.46	0.57	1.57	3.10	−0.80	0.90	standard	ρ/ρ					1.34	
	ρ/q	−3.43			2.17	−0.69		error	ρ/q					1.29	
	q/ρ	−3.74	0.75		2.19	−0.80			q/ρ					1.24	
	q/q	−4.13			2.97	−0.40			q/q					1.29	

[a] Model ρ/ρ indicates that both the reaction field $\bar{\phi}(\mathbf{r})$ and G_{RF} were calculated by using the density ρ directly. In model ρ/q, the reaction field $\bar{\phi}(\mathbf{r})$ was calculated with ρ, whereas G_{RF} was evaluated with point charges derived by ESP fitting. Model q/ρ used fitted point charges in calculating the reaction field $\bar{\phi}(\mathbf{r})$, but used charge density in evaluating G_{RF}. In model q/q, the fitted point charges were used in calculating the reaction field $\bar{\phi}(\mathbf{r})$ as well as G_{RF}. [b] G_{SAS} was calculated by multiplying the solvent-accessible surface area by 0.006. [c] G_{np} was calculated from eq 12 in which the optimized constant a was 1.53 for model ρ/ρ, 0.60 for model ρ/q, 0.62 for model q/ρ, and 1.40 for model q/q.

and the reaction field energy G_{RF} was computed by using the quantum mechanically derived charge density in eq 10. The q/ρ model has been widely used in previous mixed quantum-mechanical PB models.[5,20,21] In the q/q model, the ESP-fitted charges were used both in solving the PB equation and in calculating the reaction field energy G_{RF}.

Table 1 presents results for the relatively "simple" Cl^- ion. Experimental data for its solvation free energy was reported to vary between 73.4 and 78 kcal/mol.[42] In previous continuum solvent model calculations, the solvation free energy was found to be sensitive to the atomic charge and radius.[43] Using the ρ/ρ model, we could produce solvation energy in this range with a small van der Waals radius of 1.25 Å (solvation energy = −77.13 kcal/mol). One could see that the results obtained from the four models could be quite different. Using the charge density in solving the PB equation gave a very different reaction field from that obtained by using ESP-fitted charges. As one can see from Figure 1, the reaction field obtained by using charge density was smaller than that obtained by using ESP-fitted charges. This is because when the solute was described quantum mechanically, part of its electron density penetrated into the solvent.[18,44] With 1.25 Å as the van der Waals radius, 27% of the total electron density was lying outside in the high dielectric region. If one assumed that this portion of the charge density was entirely screened, the effective charge that generated the reaction field was smaller. One can roughly rationalize this in terms of the simple Born model for calculating the reaction field,[45]

$$\bar{\phi}(\mathbf{r}) = \frac{q}{R}\left(\frac{1}{\epsilon} - 1\right) \tag{13}$$

where R is the radius of Cl^-, ϵ is the dielectric constant of the solvent, and q is the ionic charge. The decreased effective charge reduced the reaction field. On the other hand, the charge always lied within the low dielectric region in the fixed charge model so that the full charge of magnitude one was fully appreciated. The smaller effective charge generated a smaller reaction field that distorted the electron cloud less significantly. This is also reflected in the energy G_{wfd} associated with the distortion of the electronic wave function, which was smaller when the charge density was used. It is worth pointing out that the van der Waals radius of 1.25 Å was even smaller than the radius of a Cl atom. The need to use such a nonphysical value might reflect the limitations of continuum solvent models in describing the solvation of small charged ions. As described in ref 46, continuum dielectric theory poorly describes specific solute−solvent interaction such as hydrogen bonding. As a result, continuum dielectric models often significantly underestimate the magnitude of anion solvation energies unless unphysically small cavity radii are used or explicit terms are used to model specific ion−water interactions.

On the other hand, the differences among the four models were much smaller when the models were applied to study larger molecules. Table 2 summarizes the results for 31 small neutral organic molecules. In these models, one adjustable parameter a, defined in eq 12, was used to better fit the experimental data. When the solute was described quantum mechanically, there always existed a tail of electron charge density penetrating into the high dielectric solvent that did not occur in point-charge models. As shown in Table 2, the solute wave function distortion energy G_{wfd} was slightly overestimated in the point-charge models q/ρ and q/q; however, the G_{wfd} values for butane and 1-methyluracil were quite similar for the ρ/ρ and q/ρ models. In general, a slightly weaker reaction field was generated from the full charge density model ρ/ρ because of the "leaking" of charge density into the high dielectric solvent region. When the solute experienced a weaker reaction field, its wave function was less distorted. Consequently, the value of G_{wfd} calculated from the ρ/ρ model was typically smaller than that from the q/ρ model. For these neutral molecules, about 1−2% of the electron density lied outside the molecular surface.

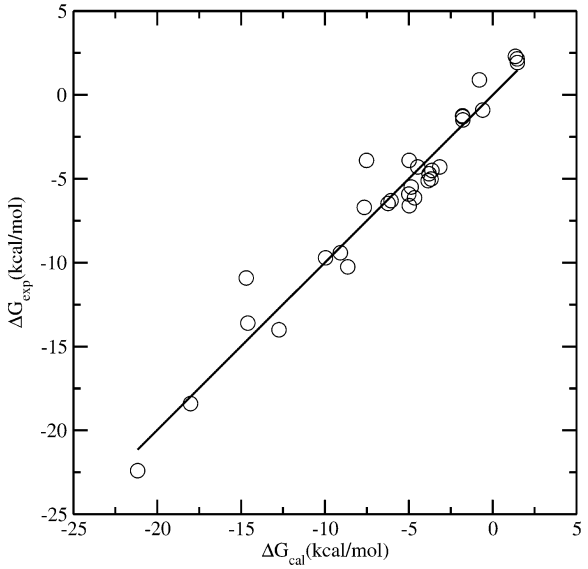

Figure 2. Correlation plot between the experimental and calculated solvation free energy using the ρ/ρ model. The correlation coefficient is 0.99.

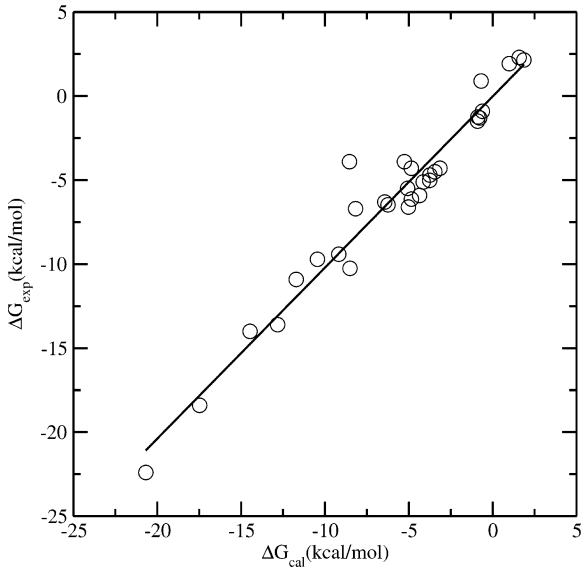

Figure 3. Correlation plot between the experimental and calculated solvation free energy using the ρ/q model. The correlation coefficient is 0.99.

To compare the calculated solvation energy with experimental data taken from refs 15 and 21, the parameter a in the term G_{np} was allowed to change to best fit the experimental results. The optimized values of a were 1.53 kcal/mol for the ρ/ρ model, 0.60 kcal/mol for the ρ/q model, 0.62 kcal/mol for the q/ρ model, and 1.40 kcal/mol for the q/q model. These values of a were close to the 1.09 value used by Honig and co-workers, who employed a similar intrinsic surface tension of 0.005 kcal/mol/A^2.[20] Although the four models were distinct by generating different reaction field energies G_{RF}, for example, one could make all four models give comparable agreement with the experimental data by allowing the parameter a to change. By doing this, we could obtain root-mean-square errors of about 1.3 kcal/mol in all four cases.

Figures 2−5 illustrate the correlation between the experimental free energies and the calculated ones from the four different models. As illustrated in Figures 2−5, the same

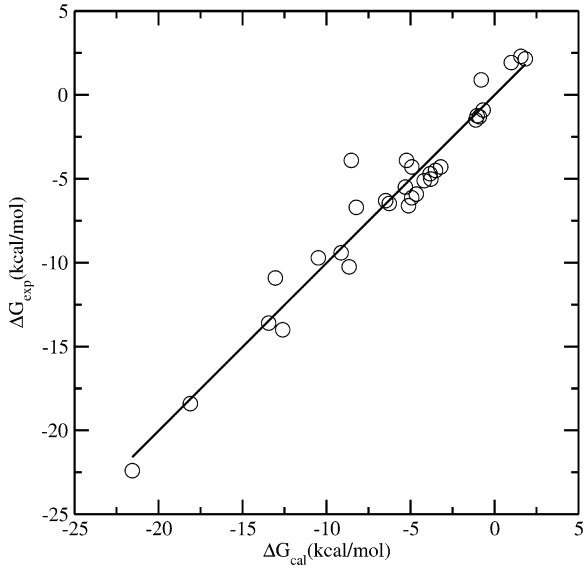

Figure 4. Correlation plot between the experimental and calculated solvation free energy using the q/ρ model. The correlation coefficient is 0.99.

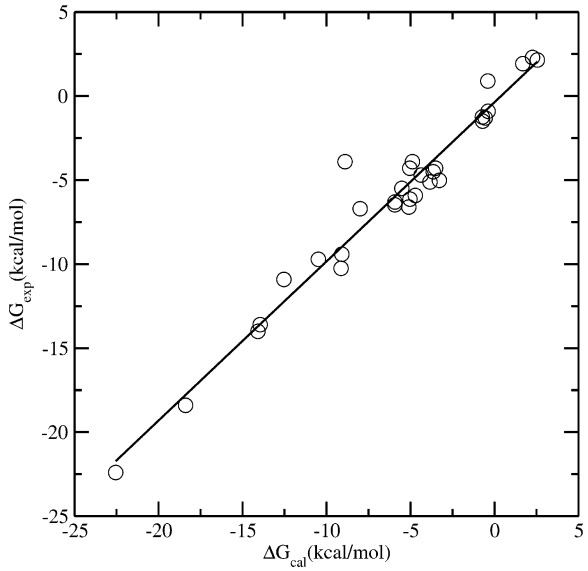

Figure 5. Correlation plot between the experimental and calculated solvation free energy using the q/q model. The correlation coefficient is 0.99.

correlation coefficient (0.99) was obtained, again indicating that all four models gave results that correlated well with experimental data for small neutral systems. Although the ρ/ρ model did not achieve better performance in calculating the solvation energy of these small neutral systems, its more physically sound representation (including better description of reaction field and wave function dispersion and distortion) may make it more appealing for other applications.

4. Conclusions

We coupled the Kohn−Sham and PB equations to explicitly take electronic polarization into account in calculating solvation free energy. We also used the more realistic dispersed-charge rather than the point-charge representation in solving the PB equation. In applying this approach to study the hydration of a chloride ion, it was necessary to use a radius much smaller than the van der Waals radius of the ion to define the dielectric boundary to obtain good agreement with the experimental data. These nonphysical results reflect the limitations of continuum solvent models in treating small charged ions. On the other hand, the results for larger molecules were much more reasonable. For the 31 small neutral molecules studied here, the model performed quite well in calculating the solvation free energy of these molecules when a single adjustable parameter was introduced to shift the calculated solvation energy. The root-mean-square deviations from the experimental results were only 1.3 kcal/mol when the solvation free energy of these molecules spanned a wide range of 25 kcal/mol. The correlation coefficient between the calculated and the experimental solvation free energy was also better than 0.99.

Acknowledgment. This research was supported in part by a Research Award from the University of Missouri-Saint Louis and a University of Missouri Research Board Award.

References and Notes

(1) Cramer, C. J.; Truhlar, D. G. *Chem. Rev.* **1999**, *99*, 2161−2200.
(2) Briggs, J. M.; Madura, J. D.; Davis, M. E.; Gilson, M. K.; Antosiewicz, J.; Luty, B. A.; Wade, R. C.; Bagheri, B.; Ilin, A.; Tan, R. C.; McCammon, J. A. *UHBD*; University of California: San Diego, CA; http://mccammon.ucsd.edu/uhbd.html.
(3) Davis, M. E.; McCammon, J. A. *J. Comput. Chem.* **1989**, *113*, 386-391.
(4) Nicholls, A.; Honig, B. *J. Comput. Chem.* **1991**, *12*, 435−45.
(5) Li, J.; Nelson, M. R.; Peng, C.-Y.; Bashford, D.; Noodleman, L. *J. Phys. Chem. A.* **1998**, *102*, 6311−6324.
(6) Baker, N. A.; Sept, D.; Joseph, S.; Holst, M. J.; McCammon, J. A. *Proc. Natl. Acad. Sci. U.S.A.* **2001**, *98*, 10037−10041.
(7) Cortis, C. M.; Langlois, J. M.; Beachy, M. D.; Friesner, R. A. *J. Chem. Phys.* **1996**, *105*, 5472.
(8) Klamt, A.; Schüürmann, G. *J. Chem. Soc., Perkin Trans.* **1993**, *2*, 799−805.
(9) York, D. M.; Lee, T.-S.; Yang, W. *Chem. Phys. Lett.* **1996**, *263*, 297−304.
(10) Miertu, S.; Scrocco, E.; Tomasi, *J. Chem. Phys.* **1981**, *55*, 117−129.
(11) Cammi, R.; Tomasi, J. *J. Comput. Chem.* **1995**, *16*, 1449−1458.
(12) Cramer, C. J.; Truhlar, D. G. *J. Am. Chem. Soc.* **1991**, *113*, 8305−8311.
(13) Bashford, D.; Case, D. A. *Annu. Rev. Phys. Chem.* **2000**, *51*, 129−152.
(14) Still, W. C.; Tempczyk, A.; Hawley, R. C.; Hendrickson, T. *J. Am. Chem. Soc.* **1990**, *112*, 6127−6129.
(15) Li, X.; Liu, H. *J. Comput. Chem.* **2002**, *23*, 1404−1415.
(16) Tomasi, J.; Persico, M. *Chem. Rev.* **1994**, *94*, 2027−2094.
(17) Orozco, M.; Luque, F. J. *Chem. Rev.* **2000**, *100*, 4187−4225.
(18) Tomasi, J.; Mennucci.; Cammi, R. *Chem. Rev.* **2005**, *105*, 2999−3093.
(19) Orttung, W. H. *J. Am. Chem. Soc.* **1978**, *100*, 4369−4375.
(20) Tannor, D. J.; Marten, B.; Murphy, R.; Friesner, R. A.; Sitkoff, D.; Nicholls, A.; Ringnalda, M.; Goddard, W. A., III; Honig, B. *J. Am. Chem. Soc.* **1994**, *116*, 11875−11882.
(21) Gogonea, V.; Merz, K. M. *J. Phys. Chem. A.* **1999**, *103*, 5171−5188.
(22) Besler, B. H.; Merz, K. M., Jr.; Kollman, P. A. *J. Comput. Chem.* **1990**, *4*, 431−439.
(23) Francl, M. M.; Chirlian, L. E. The Pluses and Minuses of Mapping Atomic Charges to Electrostatic Potentials. In *Reviews in Computational Chemistry*; Lipkowita, K. B., Boyd, D. B., Eds.; John Wiley and Sons: New York, 2000; Vol. 14.
(24) Kohn, W.; Sham, L. J. *Phys. Rev.* **1965**, *140*, A1133−1138.
(25) Baroni, S.; Dal Corso, A.; de Gironcoli, S.; Giannozzi, P.; Cavazzoni, C.; Ballabio, G.; Scandolo, S.; Chiarotti, G.; Focher, P.; Pasquarello, A.; Laasonen, K.; Trave, A.; Car, R.; Marzari, N.; Kokalj, A. PWscf Home Page. http://www.pwscf.org/ (accessed March 2006).
(26) Laasonen, K.; Pasquarello, A.; Lee, C.; Car, R.; Vanderbilt, D. *Phys. Rev. B* **1993**, *47*, 10142−10153.
(27) Giannozzi, P.; de Angelis, F.; Car, R. *J. Chem. Phys.* **2004**, *120*, 5903−5915.
(28) Payne, M. C.; Teter, M. P.; Allan, D. C.; Arias, T. A. *Rev. Mod. Phys.* **1992**, *64*, 1045−1097.
(29) Martyna, G. J.; Tuckerman, M. E. *J. Chem. Phys.* **1999**, 110, 2810−2821.
(30) Bondi, A. *J. Chem. Phys.* **1964**, *68*, 441−451.
(31) Perdew, J. P.; Burke, K.; Ernzerhof, M. *Phys. Rev. Lett.* **1996**, *77*, 3865−3868.

(32) Sharp, K. A.; Honig, B. *J. Phys. Chem.* **1990**, *94*, 7684−7692.
(33) Davis, M. E.; McCammon, J. A. *Chem. Rev.* **1990**, *90*, 509−521.
(34) Gilson, M. R.; Sharp, K. A.; Honig, B. H. *J. Comput. Chem.* **1988**, *9*, 327−335.
(35) Frisch, M. J.; Trucks, G. W.; Schlegel, H. B.; Scuseria, G. E.; Robb, M. A.; Cheeseman, J. R.; Montgomery, J. A., Jr.; Vreven, T.; Kudin, K. N.; Burant, J. C.; Millam, J. M.; Iyengar, S. S.; Tomasi, J.; Barone, V.; Mennucci, B.; Cossi, M.; Scalmani, G.; Rega, N.; Petersson, G. A.; Nakatsuji, H.; Hada, M.; Ehara, M.; Toyota, K.; Fukuda, R.; Hasegawa, J.; Ishida, M.; Nakajima, T.; Honda, Y.; Kitao, O.; Nakai, H.; Klene, M.; Li, X.; Knox, J. E.; Hratchian, H. P.; Cross, J. B.; Bakken, V.; Adamo, C.; Jaramillo, J.; Gomperts, R.; Stratmann, R. E.; Yazyev, O.; Austin, A. J.; Cammi, R.; Pomelli, C.; Ochterski, J. W.; Ayala, P. Y.; Morokuma, K.; Voth, G. A.; Salvador, P.; Dannenberg, J. J.; Zakrzewski, V. G.; Dapprich, S.; Daniels, A. D.; Strain, M. C.; Farkas, O.; Malick, D. K.; Rabuck, A. D.; Raghavachari, K.; Foresman, J. B.; Ortiz, J. V.; Cui, Q.; Baboul, A. G.; Clifford, S.; Cioslowski, J.; Stefanov, B. B.; Liu, G.; Liashenko, A.; Piskorz, P.; Komaromi, I.; Martin, R. L.; Fox, D. J.; Keith, T.; Al-Laham, M. A.; Peng, C. Y.; Nanayakkara, A.; Challacombe, M.; Gill, P. M. W.; Johnson, B.; Chen, W.; Wong, M. W.; Gonzalez, C.; and Pople, J. A. *Gaussian 03*, revision C.02; Gaussian, Inc.: Wallingford, CT, 2004.
(36) Sitkoff, D.; Ben-Tal, N.; Honig, B. *J. Phys. Chem.* **1996**, *100*, 2724−2752.
(37) Simonson, T.; Brunger, T. *J. Phys. Chem.* **1994**, *98*, 4683−4694.
(38) Ashbaugh, H. S.; Kaler, E. W.; Paulaitis, M. E. *J. Am. Chem. Soc.* **1999**, *121*, 9243−9244.
(39) Gallicchio, E.; Kubo, M. M.; Levy, R. M. *J. Phys. Chem. B.* **2000**, *104*, 6271−6285.
(40) Gallicchio, E.; Zhang, L. Y.; Levy, R. M. *J. Comput. Chem*. **2002**, *23*, 517−529.
(41) Gallicchio, E.; Levy, R. M. *J. Comput. Chem*. **2004**, *25*, 479−499.
(42) Pliego, J. R., Jr.; Riveros, J. M. *Chem. Phys. Lett.* **2000**, *332*, 597−602.
(43) Hummer, G.; Pratt, L. R.; Garcia, A. E. *J. Phys. Chem.* **1996**, *100*, 1206−1215.
(44) Chipman, D. M. *J. Chem. Phys.* **2004**, *120*, 5566−5575.
(45) Born, M. *Z. Phys.* **1920**, *1*, 45−48.
(46) Chipman, D. M. *J. Chem. Phys.* **2003**, *118*, 9937−9942.